

EMBRY-RIDDLE

Aeronautical University™

SCHOLARLY COMMONS

Publications

Summer 8-28-1998

Detection of Intergalactic Red-Giant-Branch Stars in the Virgo Cluster

Henry C. Ferguson

Space Telescope Science Institute, ferguson@stsci.edu

Ted von Hippel

University of Wisconsin, vonhippt@erau.edu

Nial R. Tanvir

University of Cambridge, nrt@ast.cam.ac.uk

Follow this and additional works at: <https://commons.erau.edu/publication>



Part of the [Stars, Interstellar Medium and the Galaxy Commons](#)

Scholarly Commons Citation

Ferguson, H. C., von Hippel, T., & Tanvir, N. R. (1998). Detection of Intergalactic Red-Giant-Branch Stars in the Virgo Cluster. *Nature*, 391(). <https://doi.org/10.1038/35087>

This Article is brought to you for free and open access by Scholarly Commons. It has been accepted for inclusion in Publications by an authorized administrator of Scholarly Commons. For more information, please contact commons@erau.edu.

Detection of Intergalactic Red Giant Branch Stars in the Virgo Cluster

Henry C. Ferguson
Space Telescope Science Institute,
Baltimore, MD 21218, USA
ferguson@stsci.edu

Nial R. Tanvir
University of Cambridge, Institute of Astronomy
Madingley Road, Cambridge CB3 0HA, UK
nrt@ast.cam.ac.uk

Ted von Hippel
Department of Astronomy, University of Wisconsin
Address: WIYN Telescope, NOAO, PO Box 26732,
Tucson, AZ 85726, USA
ted@noao.edu

August 28, 2018

It has been suspected for nearly 50 years that clusters of galaxies contain a population of intergalactic stars, ripped from galaxies during cluster formation or when the galaxies' orbits take them through the cluster center.^{1, 2, 3} Support for the existence of such a population of free-floating stars comes from measurements of the diffuse light in clusters^{4, 5, 6, 7, 8, 9}, and from recent detections of planetary nebulae with positions and/or velocities far removed from any observed cluster galaxy.^{10, 11} But estimates for the mass of the diffuse population and its distribution relative to the galax-

ies are still highly uncertain. Here we report the direct detection of intergalactic stars in deep images of a blank field in the Virgo Cluster. The data suggest that approximately 10% of the stellar mass of the cluster is in intergalactic stars. We observe a relatively homogeneous distribution of stars, with evidence of a slight gradient toward M87.

The process of cluster formation undoubtedly involved interactions and mergers of galaxies and tidal ablation of stars due to the mean gravitational shear of the cluster.² Further stripping is likely to have occurred due to “galaxy harassment”, the cumulative effect of many close, high speed encounters with massive cluster galaxies.³ Theoretical predictions for the fraction of mass in the intergalactic population range from 10% to 70%. This large uncertainty stems at a fundamental level from our poor knowledge of when galaxies formed, when and how clusters collapsed, and how the dark matter and baryonic matter were distributed within proto-galaxies.^{12, 2, 13} Detection and mapping of intergalactic stars could be an important tool for investigating these issues.

Searches for the diffuse light from intergalactic stars are extremely difficult due to the stringent requirements on background subtraction. Reported detections and upper limits range from 10% to 45% of the total cluster light in various clusters.^{6, 7, 8, 9} Even when a signal is detected, it is unclear how much is due to a true diffuse component, and how much to the extension of the galaxy luminosity function below the limits of individual source detection. Intergalactic planetary nebula candidates have been identified in the Virgo cluster (3) and the Fornax cluster (10), but these numbers are not yet sufficient to draw strong conclusions on the distribution of intergalactic stars.

In May 1996 we used the Hubble Space Telescope WFPC2 camera with the F814W (approximately I-band) filter to observe a blank field in the Virgo Cluster (Fig. 1). At faint limits compact galaxies are essentially indistinguishable from stars, so the Hubble Deep Field, which was taken in an area of sky with no foreground cluster, was used as a control. For the comparisons, the HDF images were divided into two groups, each consisting of exposures taken at three pointing positions with total exposure times identical (to within 1%) to the Virgo Cluster field. Because the sky noise was considerably lower in the HDF images, additional noise was added to match the statistics in the Virgo Cluster field. These images were re-reduced and resampled to match the Virgo Cluster images.

Figure 2 shows the comparison of source counts for the different images. Fainter than $I = 26.5$, there is a clear excess in source counts in the Virgo Cluster image. The excess amounts to approximately 630 extra sources to $I = 27.9$. We expect fewer than 20 Galactic foreground stars to this depth. The major uncertainty is the field-to-field variance in galaxy counts, because galaxies at the limiting depth of our image are only marginally resolved. For

a square field of angular size θ on a side, the expected variance in the number counts is $\Delta N^2 = N + 2.24N^2A\theta^{1-\gamma}$ where N is the mean number per field, and the angular correlation function follows the powerlaw $w(\theta) = A\theta^{1-\gamma}$.¹⁴ Using N from the HDF, and adopting $A = 1.5 \times 10^{-4}$ and $\gamma = 1.8$,¹⁵ the expected standard deviation in galaxy counts is $\Delta N = 80$, well below the 630 excess sources we detect. As a check that the HDF is not highly unusual, source detection and aperture photometry were carried out on an additional control field, centered on the radio galaxy 3C210. Source counts in this field match the HDF to within 20% down to the completeness limit ($I = 27.5$) of the 3C210 field.

The total flux from the 630 excess sources detected in the image corresponds to a total magnitude $I = 20.53$, or a surface brightness (dividing by the area of the field) of $\mu_I = 31.16$ magnitudes per square arcsecond. The source density is relatively uniform across the field, with a marginally significant gradient towards M87. To estimate the surface brightness and total mass of stars below our detection limit, consider a population with a metallicity, expressed as a decimal logarithm relative to the solar iron-to-hydrogen ratio, $[\text{Fe}/\text{H}] = -0.7$, an age of 13 Gyr, a Salpeter¹⁶ initial mass function ($N(M) \propto M^{-2.35}$), and a distance 18.2 Mpc. According to the theoretical luminosity function¹⁷ stars brighter than $M_I = -3.4$ (corresponding to a limiting magnitude $I = 27.9$ for the assumed distance) contribute 16% of the total flux from the stellar population. Our detection of 630 sources thus implies an underlying surface brightness of $\mu_I = 29.14$. The theoretical color of the population is $B - I = 1.97$, so the B -band surface brightness would be $\mu_B = 31.11$; the surface mass density would be $0.14M_\odot\text{pc}^{-2}$ if the initial mass function continues to $0.1M_\odot$.

A purely empirical estimate of the surface brightness can be made by comparison to previous HST observations of the galaxy NGC 3379.¹⁸ In those observations, approximately 39000 stars were detected in the three wide-field detectors, of which we estimate 5000 ($\pm 50\%$) were brighter than $I = 26.9$ (roughly equivalent to our detection limit in Virgo; see below). The NGC 3379 surface brightness at the radius of these observations is $\mu_B = 27.3$.¹⁹ The difference in distance moduli between NGC3379 and the Virgo Cluster is 1.0 mag.²⁰ Thus our detection of 630 stars in Virgo implies a surface brightness $-2.5 \log(630/5000) + 1.0$ magnitudes fainter, or $\mu_B = 30.6$, in reasonable agreement with the theoretical determination, given the uncertainties.

The intergalactic stars are likely to have originated primarily from the elliptical and S0 galaxies in the cluster. The early-type galaxies are more numerous in the cluster, have older stellar populations (and hence higher stellar mass-to-light ratios), and are likely to have inhabited the central megaparsec of the cluster for much longer than the spirals and irregulars.²¹ To compare the intergalactic light to the light emerging from the early-type galaxies, we divide the Virgo cluster catalog²² into successively larger annuli of 70 galaxies centered on M87 and fit mean surface brightness vs. radius, where the

mean surface brightness is the total flux from galaxies divided by the area of each annulus. This fit gives $\mu_B = 28.7$ at $r = 44.5'$. (This becomes $\mu_B = 27.9$ if spirals and irregulars are included.)

The implication is that about 10% of the stellar mass in the cluster is in the intergalactic component.

While the distinction between intracluster stars and the M87 halo becomes purely semantical at a radius of 235 kpc, it is of some interest to compare the inferred surface brightness to the extrapolated surface brightness of M87. An $r^{1/4}$ -law fit to the Caon et al. ²³ photometry between 4.2 and 9.2 arcminutes, predicts a surface brightness at $r = 44.5$ arcminutes of $\mu_B = 30.3$ along the major axis, and 33.4 along the minor axis. Our field is situated 25 degrees from the minor axis. Thus our detected number of stars is higher than expected from a pure extrapolation of the visible portion of M87. NGC 4552, located 28.8 arcmin from our field, could also contribute to the source counts. Even if we assume no tidal truncation, a fit to the minor-axis photometry from 4.3 to 6.5 arcmin predicts $\mu_B = 32.5$ at the position of our field, which would correspond to $\sim 25\%$ of the detected source density. Overlapping halos of galaxies evidently account for only a portion of the stars we detect, unless the outer profiles deviate substantially from the inner $r^{1/4}$ laws.

The estimated stellar mass fraction is sensitive to the age and metallicity of the population. For a distance modulus $(M - m)_0 = 31.3$, metallicity $[Fe/H] < -0.4$ and age > 1 Gyr, the underlying stellar mass fraction for our sample can plausibly range from 4 to 12%. At still younger ages the mass fraction goes down, while at still higher metallicities it goes up. Recent measurements of the Virgo Cluster distance modulus range from $(m - M)_0 = 31.0$ to 31.7. ^{24, 20, 25} The mass fraction is still $\sim 5 - 10\%$ unless the distance modulus is at the high end of this range *and* the metallicity is greater than $[Fe/H] = -0.7$.

The present observations thus favor a rather small mass fraction in the diffuse population. In contrast, Theuns and Warren ¹¹ infer from the detection of 10 planetary nebula candidates, that 40% of the stellar mass is in the diffuse population of the Fornax Cluster. ¹¹ Our results are consistent only if the intergalactic population is metal-rich, or the Virgo Cluster is more distant than ~ 20 Mpc. However, the planetary-nebula estimate suffers from small number statistics, possible contamination of the sample by background emission-line galaxies, and variations in the planetary-nebula specific frequency with stellar population.

For an assumed distance of 18.2 Mpc, the total gravitating mass estimated from X-ray observations in the central 240 kpc of the Virgo Cluster is $1.2 - 3.5 \times 10^{13} M_\odot$, ²⁶ and the corresponding mass to light ratio $M/L_B \approx 260$. Most of the *light* in the central region of the Virgo Cluster resides in the central 10' of M87, while most of the *mass* resides at larger radii. For the region outside this central 10', our observations imply a mean $M/L_B \approx 700$. The relatively

smooth distribution of mass inferred from the X-ray observations²⁶ suggests that most of the intergalactic material was stripped via tidal interactions with the cluster potential, although we cannot rule out the possibility that some of the stars formed *in situ*, or that some were stripped off by impulsive interactions between galaxies (“harassment”).

The luminosity of the tip of the red giant branch has been promoted as a distance indicator of comparable precision to Cepheid variables.²⁷ While the number of stars in our sample is not large enough for a precise distance estimate, the shape of the observed luminosity function is consistent with that seen in the halo of NGC 5128²⁸, and in the halo of NGC 3379¹⁸, shifted to a distance modulus in the range $31.2 < (m - M)_0 < 31.6$.

Future observations should reveal whether the profile of the intergalactic stars is similar to that of the gravitating mass, whether it is centered on M87, and whether it is smoothly distributed. The new instruments on HST make it possible to measure the metallicity distribution of the diffuse stellar population and compare it to the metallicity distribution in the outer parts of elliptical galaxies and in the X-ray gas. Star counts also open the possibility of measuring the tidal radii of galaxies in the Virgo Cluster, and searching for the wakes of galaxies moving through the intracluster material. The combination of HST imaging and ground-based detection of planetary nebulae provides a powerful new probe of the cluster environment and of this nearly invisible population of stars.

References

1. F. Zwicky, The Coma cluster of galaxies, *Publ. Astron. Soc. Pac.* **63**, 61–71, (1951).
2. D. Merritt, Relaxation and tidal stripping in rich clusters of galaxies. ii - evolution of the luminosity distribution, *Astrophys. J.* **276**, 26–37, (1984).
3. B. Moore, N. Katz, G. Lake, A. Dressler, and A. J. Oemler, Galaxy harassment and the evolution of clusters of galaxies, *Nature* **379**, 613–616, (1996).
4. G. de Vaucouleurs, The apparent density of matter in groups and clusters of galaxies, *Astrophys. J.* **131**, 585–597, (1960).
5. J. E. Gunn, Visual background radiation in the coma cluster of galaxies, *BAAS* **1**, 191, (1969).
6. T. X. Thuan and J. Kormendy, Photographic measurements of diffuse light in the Coma cluster, *Publ. Astron. Soc. Pac.* **89**, 466–473, (1977).
7. J. Uson *et al.*, Diffuse light in dense clusters of galaxies. i - R-band observations of abell 2029, *Astrophys. J.* **369**, 46–53, (1991).

8. R. Vilchez-Gomez *et al.*, Detection of intracluster light in the rich clusters of galaxies Abell 2390 and CL1613+31, *Astron. Astrophys.* **283**, 37–50, (1994).
9. X. Scheick and J. R. Kuhn, Diffuse light in A2670: Smoothly distributed?, *Astrophys. J.* **423**, 566–580, (1994).
10. M. Arnaboldi *et al.*, The kinematics of the planetary nebulae in the outer regions of NGC 4406, *Astrophys. J.* **472**, 145–152, (1996).
11. T. Theuns and S. J. Warren, Intergalactic stars in the Fornax cluster, *Mon. Not. R. Astron. Soc.* **284**, L11–L15, (1996).
12. G. E. Miller, Effects of galaxy collisions on the structure and evolution of galaxy, *Astrophys. J.* **268**, 495–512, (1983).
13. B. Moore, N. Katz, and G. Lake, On the destruction and overmerging of dark halos in dissipationless n-body simulations, *Astrophys. J.* **457**, 455–459, (1996).
14. P. J. E. Peebles, Statistical analysis of catalogs of extragalactic objects vi. the galaxy distribution in the Jagellonian field, *Astrophys. J.* **196**, 647–652, (1975).
15. T. G. Brainerd, I. Smail, and J. Mould, The evolution in clustering of galaxies to $R=26$, *Mon. Not. R. Astron. Soc.* **275**, 781–789, (1995).
16. E. E. Salpeter, The luminosity function and stellar evolution, *Astrophys. J.* **121**, 161–167, (1955).
17. G. Bertelli, A. Bressan, C. Chiosi, F. Fagotto, and E. Nasi, Theoretical isochrones from models with new radiative opacities, *Astron. Astrophys. Supp.* **106**, 275–302, (1994).
18. S. Sakai, B. Madore, W. L. Freedman, T. R. Lauer, E. A. Ajhar, and W. A. Baum, Detection of the tip of the red giant branch in NGC 3379 (M105) in the Leo I group using the Hubble Space Telescope, *Astrophys. J.* **478**, 49–57, (1997).
19. M. Capaccioli, E. V. Held, H. Lorenz, and M. Vietri, Photographic and CCD surface photometry of the standard elliptical galaxy NGC3379, *Astron. J.* **99**, 1813–1822, (1990).
20. N. R. Tanvir, T. Shanks, H. C. Ferguson, and D. R. T. Robinson, Determination of the Hubble constant from observations of Cepheid variables in the galaxy M96, *Nature* **377**, 27–31, (1995).
21. R. B. Tully and E. J. Shaya *Astrophys. J.* **281**, 31, (1984).
22. B. Binggeli, A. Sandage, and G. A. Tammann, Studies of the Virgo cluster. ii – a catalog of 2096 galaxies in the Virgo cluster area, *Astron. J.* **90**, 1681–1771, (1985).

23. N. Caon, M. Capaccioli, and R. Rampazzo, Photographic and CCD surface photometry of 33 early-type galaxies in the Virgo cluster, *Astron. Astrophys. Supp.* **86**, 429–471, (1990).
24. W. L. Freedman, B. F. Madore, J. R. Mould, R. Hill, L. Ferrarese, R. C. Kennicutt, A. Saha, P. B. Stetson, J. A. Graham, H. Ford, J. G. Hoessel, J. Huchra, S. M. Hughes, and G. D. Illingworth, Distance to the Virgo cluster galaxy M100 from Hubble Space Telescope observations of Cepheids, *Nature* **371**, 757–762, (1994).
25. A. Sandage and G. Tammann, An alternative calculation of the distance to M87 using the Whitmore et al. luminosity function for its globular clusters: H_0 therefrom, *Astrophys. J. Lett.* **464**, L51–L54, (1996).
26. P. E. J. Nulsen and H. Böhringer, A Rosat determination of the mass of the central Virgo cluster, *Mon. Not. R. Astron. Soc.* **274**, 1093–1106, (1995).
27. M. G. Lee, W. L. Freedman, and B. F. Madore *Astrophys. J.* **417**, 553–559, (1993).
28. R. Soria, J. R. Mould, A. M. Watson, J. S. I. Gallagher, G. A. Ballaster, C. J. Burrows, S. Casertano, J. T. Clarke, D. Crisp, R. E. Griffiths, J. J. Hester, J. G. Hoessel, J. A. Holtzman, P. A. Scowen, K. R. Stapelfeldt, J. T. Trauger, and J. A. Westphal, Detection of the tip of the red giant branch in NGC5128, *Astrophys. J.* **465**, 79–90, (1996).
29. J. A. Holtzman, C. J. Burrows, S. Casertano, J. J. Hester, J. T. Trauger, A. M. Watson, and G. Worthey, The photometric performance and calibration of WFPC2, *Publ. Astron. Soc. Pac.* **107**, 1065–1093, (1995).
30. D. Burstein and C. Heiles, Reddening estimates for galaxies in the second reference catalog and the Uppsala general catalog, *Astrophys. J. Supp.* **54**, 33–79, (1984).
31. R. E. Williams, B. Blacker, M. Dickinson, W. V. D. Dixon, H. C. Ferguson, A. S. Fruchter, M. Giavalisco, R. L. Gilliland, I. Heyer, R. Katsanis, Z. Levay, R. Lucas, D. McElroy, L. Petro, M. Postman, H.-M. Adorf, and R. N. Hook, The Hubble deep field: Observations, data reduction, and galaxy photometry, *Astron. J.* **112**, 1335–1389, (1996).

Methods

The zero-point of the instrumental magnitude scale was established by measuring the fluxes of the few bright isolated stars in the field in $0.5''$ radius apertures following the standard prescription. ²⁹ Additional corrections were made as follows: (a) +0.05 mag to correct for the so-called “long exposure” effect (Hill et al. in press); (b) –0.04 mag, which is the appropriate color term

to convert to standard Cousins's I magnitudes for red stars with $V-I \sim 1.5$;²⁹ and (c) -0.04 mag to allow for the expected foreground extinction.³⁰ We estimate that the combined uncertainty from the zero-point calibration and the various correction terms amounts to 0.06 mag. Clearly extended sources were removed from the catalog by restricting our analysis to sources with a DAOPHOT sharpness parameter $-0.6 < s < 0.4$. A similar procedure was also followed for the HDF control field. Finally, we created 12 test data-sets in which 265 simulated stars were added to the real data frames. The input magnitudes of the simulated stars covered the range from 23.5 to nearly 30. We then processed these frames in the same way as the original data and produced a matrix relating the recovered magnitudes and detection efficiency to the input magnitudes of the simulated stars. From these simulations we estimate that the catalog is $\sim 80\%$ complete at $I = 27.9$, and use this as the limiting magnitude in our analysis.

Acknowledgments

We are grateful to Shoko Sakai, Roberto Soria, and Carl Grillmair for providing stellar photometry from nearby galaxies for comparison to the Virgo Cluster data, to Mark Dickinson for the use of the 3C210 comparison field, and to Andy Fruchter and Richard Hook for use of the drizzle code. We would also like to thank Vera Rubin, Francois Schweizer, and Abi Saha for helpful discussions and the Department of Terrestrial Magnetism for hospitality (TvH). TvH was partially supported by a grant from the Edgar P. and Nona B. McKinney Charitable Trust. Support for this work was also provided by NASA through a General Observer research grant awarded by Space Telescope Science Institute, which is operated by the Association of Universities for Research in Astronomy.

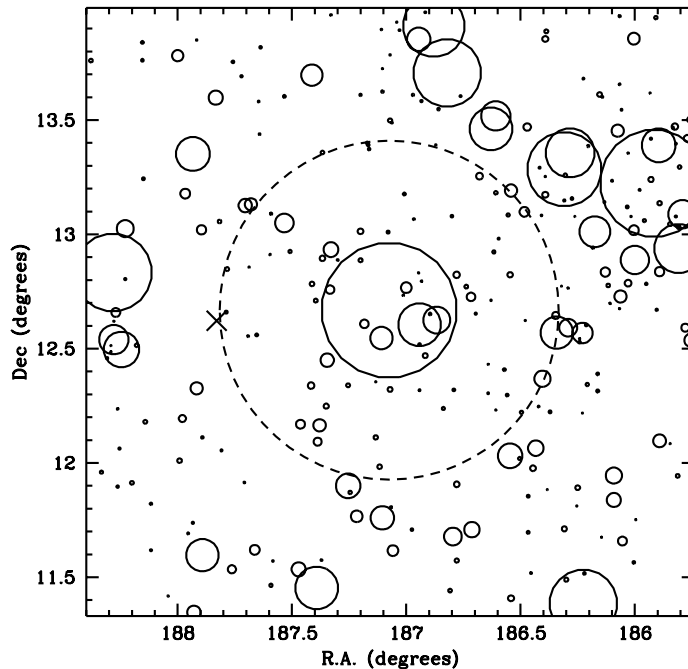


Figure 1:

The 'X' marks the position of the HST images in this view of the core of the Virgo Cluster. The solid circles mark positions of cluster galaxies, and are scaled by the square root of the galaxy luminosity. The central bright galaxy is M87, and the dashed circle marks a region 44.5 arcminutes from M87. The field is located on this circle ~ 235 kpc east of M87 (J2000 coordinates $12^h 33^m 52^s$, $12^\circ 21' 40''$) and well separated from any of the other bright galaxies in the cluster (Figure 1). The WFPC2 field covers 5.33 square arcminutes. The nearest galaxy to the WFPC field is a dE galaxy with a magnitude $B=18.0$, $6.6'$ away. The nearest bright galaxy is NGC 4552 ($B = 10.8$), at a distance of $23'$ ($= 122$ kpc if the distance to the Virgo Cluster is 18.2 Mpc). The total exposure time for the observation was 33500 seconds. The exposures were taken at three positions separated by $\pm 0.33''$ to improve resolution and aid in removing hot pixels and other cosmetic defects. Data were reduced and images combined following the procedures for the Hubble Deep Field (HDF).³¹ The final reduced images were resampled via "drizzling" (Fruchter and Hook 1997, in preparation) onto a pixel grid of $0.08''$.

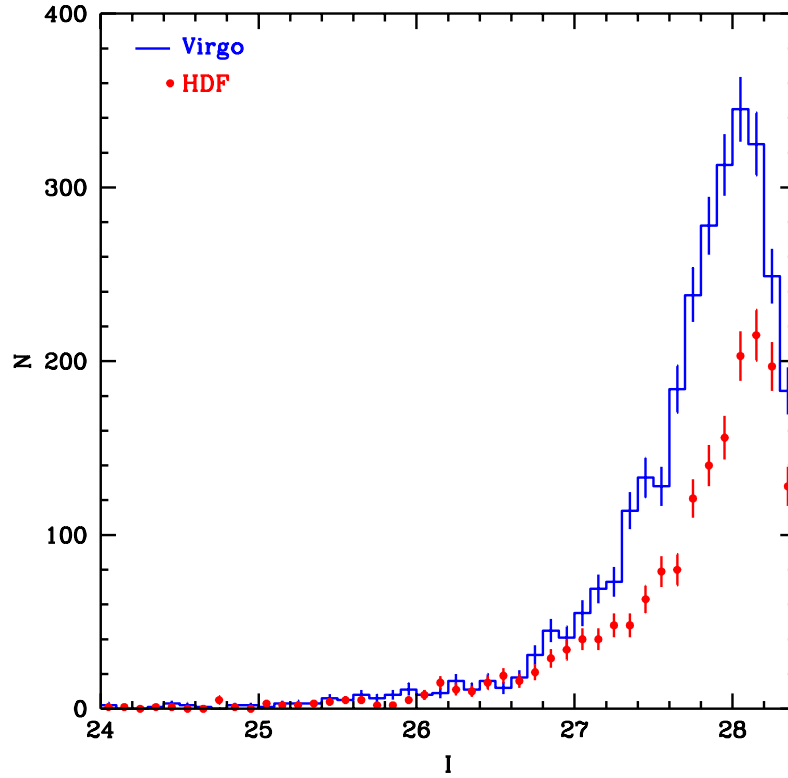


Figure 2:

Comparison of source counts in the Virgo Cluster field and the HDF. The histogram is the Virgo Cluster field. The points with error bars are the HDF. Magnitudes are based on PSF fitting. The excess in the Virgo Cluster field begins at $I \approx 26.8$. Source detection was performed using DAOFIND, and profile-fitting photometry was performed with the IRAF implementation of the DAOPHOT ALLSTAR code. See Methods for further details.